

Theory of first-order layering transitions in thin helium films

W. M. Saslow and G. Agnolet

Center for Theoretical Physics and Department of Physics, Texas A&M University, College Station, Texas 77843

C. E. Campbell

School of Physics and Astronomy, University of Minnesota, Minneapolis, Minnesota 55455

B. E. Clements

Center for Theoretical Physics and Department of Physics, Texas A&M University, College Station, Texas 77843;
Los Alamos National Laboratory, Los Alamos, New Mexico 87545;
and Institut Laue Langevin, 38042 Grenoble Cedex, France

E. Krotscheck

Center for Theoretical Physics and Department of Physics, Texas A&M University, College Station, Texas 77843
and Institut für Theoretische Physik, Johannes Kepler Universität Linz, A-4040 Linz, Austria

(Received 12 March 1996)

Thin liquid ^4He films on graphite show evidence of layered growth with increasing number density via a succession of first-order phase transitions. These so-called “layering transitions” separate uniformly covering phases, such as monolayers and bilayers. The present work is a detailed theoretical study of such layering transitions using a Maxwell construction. We model the graphite surface by a strong substrate potential, and using a microscopic variational theory we obtain the uniform coverage solutions for liquid helium. For each layer, the theory yields the chemical potential μ and surface tension α as functions of coverage n , and from this we deduce $\mu(\alpha)$. For each set of adjacent layers, we then obtain the crossing point in the curves of $\mu(\alpha)$. In this way we obtain the values of μ , α , and surface coverages for the transition. Particular attention is paid to the monolayer-bilayer transition. [S0163-1829(96)01933-9]

I. INTRODUCTION

The properties of thin ^4He films, for a wide range of coverages and temperatures, have been studied experimentally for many years. Techniques such as specific heat,^{1,2} third sound,³ neutron scattering,⁴ nuclear magnetic resonance,⁵ and torsional oscillator measurements⁶ have all been used to determine the structure and behavior of this system. There is considerable evidence^{1,4,7,8} that liquid ^4He arranges itself in well-defined atomic layers parallel to the substrate. The transition between films of different thickness is not necessarily continuous, but can happen discontinuously through a succession of phase transitions, called *layering transitions*.

Theoretical work has yielded results^{9–13} consistent with a succession of such discontinuous, or first-order, phase transitions. These layering transitions typically occur near layer completion. They separate a uniformly covering phase from a phase where two-dimensional (2D) clusters are adsorbed onto helium underlayers. Layering transitions have been discussed theoretically for many years: De Oliveira and Griffiths⁹ discuss them for classical systems using a lattice-gas model; a general discussion of the effect of substrate strength and range on multilayer growth, including layering transitions, may be found in Ref. 10. The first quantum-mechanical theory predicting layering transitions was given in Refs. 11 and 12, using the variational method, and was later verified by path-integral Monte Carlo calculations.¹³ However, although layering transitions have been predicted,

no previous work, to our knowledge, discusses the phase-separation boundary in detail.

The present paper is devoted to a detailed study of layering transitions for ^4He , concentrating on the monolayer-bilayer case. For the requisite Maxwell construction, we employ input from existing microscopic calculations of the energy per particle, ϵ , and the chemical potential μ , as functions of surface coverage n .

It is not *a priori* obvious that layering transitions should occur for higher liquid layers in a multilayer ^4He film; nor is it clear that such transitions can occur on any substrate. Typically, the variational method finds that strong, steep substrate potentials (as for graphite and glass) favor layering transitions, whereas the shallower, longer-range substrate potentials (as for alkali metals) tend to suppress layering transitions.¹⁴ This agrees with the general considerations of Ref. 10.

In the present work, we consider a substrate potential appropriate to graphite, and model only those *fluidlike* layers in excess of what is required to produce the first two solid layers. These layers are sufficiently far from the graphite surface that they are not affected by the surface corrugation and other nonintrinsic surface irregularities or inhomogeneities. In addition to being influenced by the substrate, the properties of thin ^4He films are influenced by many-body phenomena reflecting the hard-core helium-helium interaction.

Layering transitions *may* occur when there are two locally stable uniform states of the helium film for a range of surface coverages n . The Maxwell construction determines the cov-

erages for each state at which the system starts to go from one state to the other. With α denoting the surface tension, the locus in α - n space of these *coexistence points* for different temperatures defines the *coexistence line*.

Layering transitions *must* occur when there is a range of surface coverages where the system is unstable to uniform compression. The onset of this instability is signaled by the vanishing of the third-sound velocity c_3 .^{11,12} Third sound corresponds to a areal density excitation — that is, a surface mode — propagating parallel to the liquid-vacuum interface of the film. The corresponding locus of instability points, or *spinodal points*, defines the *spinodal line*. The spinodal line lies within the coexistence line, serving to define the limits of metastability.

The treatment of the solid layers and the physical assumptions implicit to this model have been discussed earlier.^{11,12} Section II summarizes the microscopic theory employed to provide the necessary macroscopic properties. Section III discusses the direct Maxwell construction by which we determine the chemical potential and surface tension at which the transition takes place. It also discusses the determination of the spinodal points, and the tangent method of performing the Maxwell construction. Although the direct method we employ is equivalent to the tangent method of Maxwell, the direct method is more suited to the output provided by the present microscopic theory. Section IV employs the results from the microscopic variational calculations to actually perform the Maxwell construction. It also presents a full discussion of what happens as helium is added to the system, to obtain the monolayer-bilayer equilibrium coexistence line that describes the layering transition. A substantial regime of surface coverage may be metastable, thus enhancing the likelihood of experimentally observing the layering transition. Section V discusses some experimental consequences of layering transitions. Section VI provides a brief summary and our conclusions.

II. THEORETICAL BACKGROUND

Theoretical methods to study ^4He films include microscopic variational theory,^{15,12} quantum Monte Carlo theory,¹³ and density functional theory.¹⁶ Of these, the microscopic variational theory^{15,12} is particularly well suited for studies of inhomogeneous films because it is not hampered by finite-size or limited-sampling effects; nor is it influenced by biases implicit in the fitting functionals. For that reason, we have employed it to obtain the requisite microscopic information about this system.

With constantly improving computational facilities, the more detailed variational theory and quantum Monte Carlo theory become less demanding to implement. Both of these methods give not only the energies and densities, but also the two-body correlation functions. These two methods are essentially complementary in their strengths and weaknesses. The quantum Monte Carlo theory is more accurate but more time consuming, but its results contain statistical fluctuations, whereas the approximate variational method is faster and without statistical fluctuations, but needs a comparison with exact results to demonstrate its validity.

In recent years a consensus has been reached on a “generic” microscopic theory for strongly interacting particles,

in the sense that the major theoretical methods — variational method,¹⁷ the Feynman-diagram-based parquet-diagram theory,¹⁸ and the coupled cluster theory¹⁹ — all lead to the same set of many-body equations to be solved, namely, the hypernetted-chain Euler-Lagrange equations derived by Campbell and Feenberg.^{17,20} In fact, the same set of equations can also be obtained from an augmentation of density functional theory if minimal information on short-range correlations is implemented.²¹ Hence, the actual means of derivation is a matter of taste, but not of substance. We now present a brief summary of the variational method, as applied to inhomogeneous systems. A complete description may be found in Ref. 15, and further details on the three-body equations are discussed in Ref. 12.

The only input to the theory is the microscopic Hamiltonian

$$H = \sum_i^N \left[-\frac{\hbar^2}{2m} \nabla_i^2 + U_{\text{sub}}(\mathbf{r}_i) \right] + \sum_{i<j}^N V(|\mathbf{r}_i - \mathbf{r}_j|), \quad (2.1)$$

where m is the ^4He mass, $V(|\mathbf{r}_i - \mathbf{r}_j|)$ is the ^4He - ^4He interaction,²² and $U_{\text{sub}}(\mathbf{r})$ is the ^4He -substrate potential.

The variational method begins with an ansatz for the ground-state wave function of the form

$$\Psi_0(\mathbf{r}_1, \dots, \mathbf{r}_N) = \exp \frac{1}{2} \left[\sum_i u_1(\mathbf{r}_i) + \sum_{i<j} u_2(\mathbf{r}_i, \mathbf{r}_j) + \sum_{i<j<k} u_3(\mathbf{r}_i, \mathbf{r}_j, \mathbf{r}_k) \right]. \quad (2.2)$$

The correlation functions $u_1(\mathbf{r}_i)$, $u_2(\mathbf{r}_i, \mathbf{r}_j)$, and $u_3(\mathbf{r}_i, \mathbf{r}_j, \mathbf{r}_k)$ have intuitively simple physical interpretations: For example, $u_1(\mathbf{r}_i)$ reflects the broken symmetry of the system, disappearing in the homogeneous limit, and $u_2(\mathbf{r}_i, \mathbf{r}_j)$ predominantly reflects the core exclusion principle, which turns out to be the driving mechanism for the layered growth of the film. Note also that $u_2(\mathbf{r}_i, \mathbf{r}_j)$ and all derived two-body quantities, such as the two-body density or the pair distribution function, reflect the full symmetry breaking of the system. For the present planar geometry, they are functions of z_1 , z_2 , and r_{\parallel} , where z_1 and z_2 are the distances of the two particles from the substrate, and r_{\parallel} their relative distance parallel to the surface.

The correlation functions $u_n(\mathbf{r}_1, \dots, \mathbf{r}_n)$ are determined by the condition such that they minimize the ground-state energy E :

$$\frac{\delta E}{\delta u_n(\mathbf{r}_1, \dots, \mathbf{r}_n)} = 0. \quad (2.3)$$

In practice, the energy expectation value and the Euler equation (2.3) are evaluated using the hypernetted chain (HNC) hierarchy of integral equations. An important consideration in that procedure is that an *approximate* energy functional reflects the features of the *exact* energy functional. Among numerous desirable properties, the Euler equations have no solutions if the assumed symmetry of the state is physically unstable.²³ Hence this method cannot provide information about the unphysical region employed in the equal-areas approach to the Maxwell construction. The Maxwell construction in this case must be obtained either by the tangent

method or a direct approach, using results applicable in the regime where the system is stable. Both methods are discussed in the next section.

In principle, the only limitations on the variational method arise from its truncation of the wave function at the level of triplet correlations and the computational effort to determine the relevant “elementary” diagrams. These diagrams arise in the theory when the hypernetted-chain equations are invoked as part of a tractable scheme for solving the Euler equations. Applied to the bulk liquid, the most recent implementations^{24,25} of the theory reproduces the equation of state over a wide density range, with the ground-state energy given to better than 0.02 K. When compared with the 2D Monte Carlo calculations of Refs. 26 and 27, the method is similarly successful in two dimensions.

Our model of the substrate includes contributions from the two solidlike layers of helium and from the graphite substrate; details of the substrate potential can be found in Ref. 12. The ground state is completely determined for any choice of surface coverage by specifying the substrate potential, the ⁴He-⁴He interaction, and the surface coverage n . Calculation using the variational method then yields the energy per particle, ϵ , and the chemical potential μ , the speed of sound, the density profiles $\rho(z)$, and the Feynman excitation spectra as a function of the surface coverage n .

III. THERMODYNAMICS, MAXWELL CONSTRUCTION, AND SPINODAL POINTS

We first review the Maxwell construction for a bulk system. There, the thermodynamics is specified by the differential form for the total energy:

$$dE = TdS - PdV + \mu dN. \quad (3.1)$$

The equilibrium conditions for a single-component system are that the temperature T , pressure P , and chemical potential μ be uniform throughout the system. If more than one phase can exist at a given pressure and temperature, then the equilibrium phase is the one with the smallest chemical potential. At a fixed temperature, the equilibrium phase can be different for different pressures. In such cases the two chemical potential curves $\mu_1(P)$ and $\mu_2(P)$ must cross at the coexistence pressure P^* , where

$$\mu^* = \mu_1(P^*) = \mu_2(P^*). \quad (3.2)$$

At this pressure, the system goes from the low-density phase to the high-density phase as the average density is increased. These two densities define the *coexistence points*. Thus the two phases coexist over a range of *average* densities for which neither phase is individually stable.

In addition, when the system is metastable, each phase can extend beyond its coexistence point until it reaches a *spinodal point*, where the bulk compressibility

$$-\frac{1}{V} \left(\frac{\partial V}{\partial P} \right) \Bigg|_T$$

diverges. At this density, the system must undergo a first-order phase transition.

By analogy to the bulk, the energy of a surface system has the differential

$$dE = TdS + \alpha dA + \mu dN. \quad (3.3)$$

Here α is the surface tension (or surface energy per unit area) and A is the surface area.

In this case the equilibrium conditions for a single-component system are that the temperature, surface tension, and chemical potential be uniform throughout the system. As for the bulk system, two phases can coexist at a given temperature if at some surface tension α they have a common chemical potential

$$\mu^* = \mu_1(\alpha^*) = \mu_2(\alpha^*). \quad (3.4)$$

At this surface tension, the system goes from the low-density phase to the high-density phase as the average density is increased. These two densities define the *coexistence points*. Thus the phases coexist over a range of *average* densities for which neither phase is individually stable.

In practice, the zero-temperature variational theory yields the energy per particle, $\epsilon = E/N$, and μ as a function of the surface density $n = E/A$ for each layer. The surface density n is obtained from the one-body number density ρ_1 integrated over the width of the film, $n = \int dz \rho_1(z)$, and it does not include the atoms within the first two solid layers. For the Maxwell construction, we need α . To obtain it from this input requires some minor formal development.

From Eq. (3.3), at fixed A one has

$$\mu = \frac{\partial E}{\partial N} = \frac{\partial(N\epsilon)}{\partial N} = \frac{\partial(nA\epsilon)}{\partial(nA)} = \frac{\partial(n\epsilon)}{\partial n} = \epsilon + n \frac{\partial\epsilon}{\partial n} \quad (3.5)$$

and at fixed N one has

$$\alpha = \frac{\partial E}{\partial A} = \frac{\partial(N\epsilon)}{\partial(N/n)} = \frac{\partial\epsilon}{\partial n^{-1}} = -n^2 \frac{\partial\epsilon}{\partial n} = n(\epsilon - \mu). \quad (3.6)$$

From (ϵ, μ, n) and Eq. (3.6), for each layer one can immediately obtain α . Then, for each layer one plots both α and μ vs n , from which one determines $\mu(\alpha)$ for each layer. The Maxwell construction, Eq. (3.4), can then be performed directly to obtain the coexistence points. Although the ground-state structure of the liquid film was calculated over a much wider range of coverages, we will focus in the present work only on those coverages for which the layering transitions are most pronounced.

In addition to the two coexistence points, there are also two spinodal points, at which the surface compressibility

$$-\frac{1}{A} \left(\frac{\partial A}{\partial \alpha} \right) \Bigg|_T$$

diverges. Explicitly, using the Gibbs-Duhem relation

$$Nd\mu = -SdT - A d\alpha, \quad (3.7)$$

the surface compressibility is

$$\begin{aligned} \frac{1}{A} \left(\frac{\partial A}{\partial \alpha} \right) \Bigg|_{T,N} &= -\frac{1}{A} \left(\frac{\partial A}{(N/A)\partial\mu} \right) \Bigg|_{T,N} = -\frac{1}{N} \left(\frac{\partial(N/n)}{\partial\mu} \right) \Bigg|_{T,N} \\ &= \frac{1}{n^2} \left(\frac{\partial n}{\partial\mu} \right) \Bigg|_T. \end{aligned} \quad (3.8)$$

We will find it convenient to express the reciprocal compressibility in terms of the third-sound velocity. To see this, note that for a uniform system with mass density ρ the sound velocity c is given by $c^2 = \partial P / \partial \rho$. Correspondingly, by letting $(P, \rho) \rightarrow (-\alpha, mn)$ we see that the third-sound velocity should be given by $c_3^2 = -\partial \alpha / \partial (mn)$. Use of Eqs. (3.5) and (3.6) then permits us to write

$$mc_3^2 = n \frac{\partial \mu}{\partial n}. \quad (3.9)$$

Thus, to determine the spinodal points, one can either take $\partial \mu / \partial n$ numerically, using two different values of n , or one can determine c_3 at a given value of n . In practice, to avoid numerical uncertainties¹² that can occur when taking the thermodynamic derivative of μ at different n , c_3 is deduced from the excitation spectrum at a given n , and then $\partial \mu / \partial n$ is calculated from Eq. (3.9) rather than from Eq. (3.8). In general, these two calculations of c_3 will agree only for an exact theory.

Alternatively to the direct Maxwell construction, one can perform the tangent Maxwell construction. This is based upon drawing tangent lines y to the curves of ϵ vs n^{-1} , for two adjacent layers, and finding the densities at which the two tangent lines coincide. Using Eqs. (3.5) and (3.6), it is straightforward to show that, if y denotes the tangent line at a point 1, then

$$y = \epsilon_1 + \frac{\partial \epsilon}{\partial n^{-1}} (n^{-1} - n_1^{-1}) = \mu_1 + \alpha_1 n^{-1}. \quad (3.10)$$

Since matching of both the chemical potential μ and the surface tension α must occur for two layers to coexist when tangent lines for two layers coincide, these matching conditions are satisfied at the coexistence points.

For the bulk, the corresponding equation for the tangent line is

$$y = \epsilon_1 + \frac{\partial \epsilon}{\partial \rho^{-1}} (\rho_1^{-1} - \rho^{-1}) = \mu_1 - P_1 \rho^{-1}. \quad (3.11)$$

IV. RESULTS OF CALCULATION

A. Overview

We have studied the first three liquid overlayers in detail. Each overlayer can be described with a set of points (a, b, c, d) , as shown in Fig. 1. Points a and d define the limits of local stability of each layer: At a the uniform solution becomes locally stable on increasing the number density, and at d it becomes locally unstable on increasing the the number density. At these spinodal points, the surface compressibility is infinite and $c_3 = 0$, as shown in Fig. 2, which presents c_3 for each layer.

Unlike points a and d , the points b and c are not intrinsic to the layer. They are the points where a Maxwell construction must be made in order to determine the range of coverages of coexistence from one layer to another. The points b correspond to the high-coverage side of the transition, and the points c give the low-coverage side. In the case of the first layer, point b_1 is given only schematically. It cannot be determined from our calculation because the true lower-

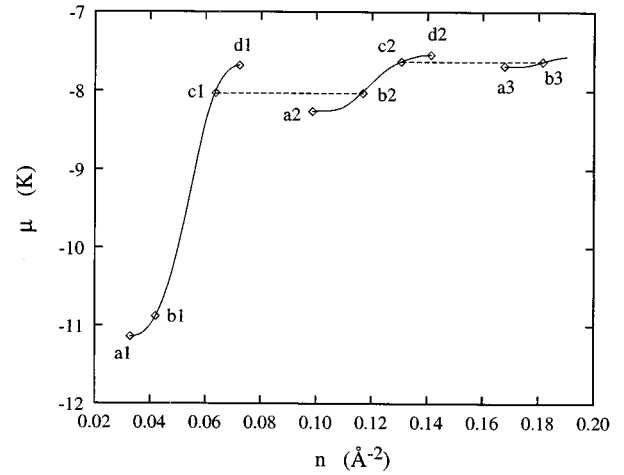


FIG. 1. The variational theory chemical potential for the mono-layer and bilayer ^4He film. The horizontal dotted lines c_1 - b_2 and c_2 - b_3 are the two-phase coexistence regions obtained from the Maxwell construction.

coverage state has two solid layers, whereas we have approximated the substrate as inert. To be specific, we have placed point b_1 at the zero-pressure coverage for the mono-layer. The true position of b_1 is likely to fall between this value and a_1 . On the other hand, points c_1 and b_2 , describing the coexistence regime for the (first-order) monolayer-bilayer transition, are determined from the Maxwell construction described in the previous section. Points c_2 and d_2 are similar to c_1 and d_1 , and points a_3 and b_3 are similar to a_2 and b_2 .

In the case of uniformly covering layers, true equilibrium occurs only between adjacent points b and c . In Fig. 1, between adjacent points a and b , and between c and d , the uniformly covering film is metastable. The horizontal dashed lines give the equilibrium values of the chemical potential; the segment c_1 and b_2 , for example, corresponds to coexistence of a nearly completed monolayer and the forming

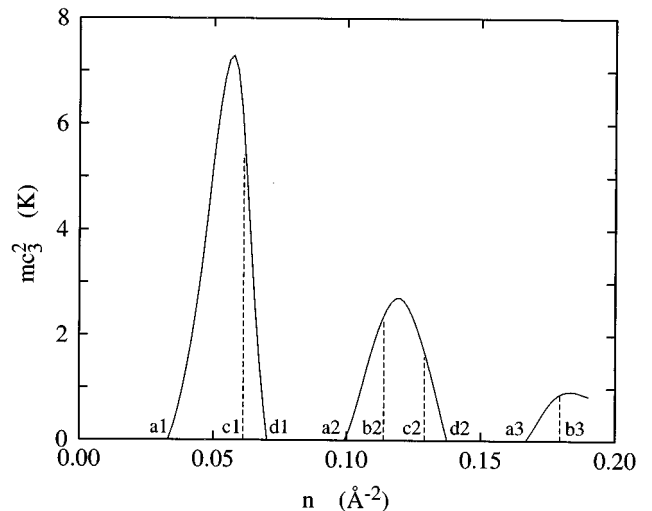


FIG. 2. The theoretical reciprocal compressibility mc_3^2 for the ^4He liquid film.

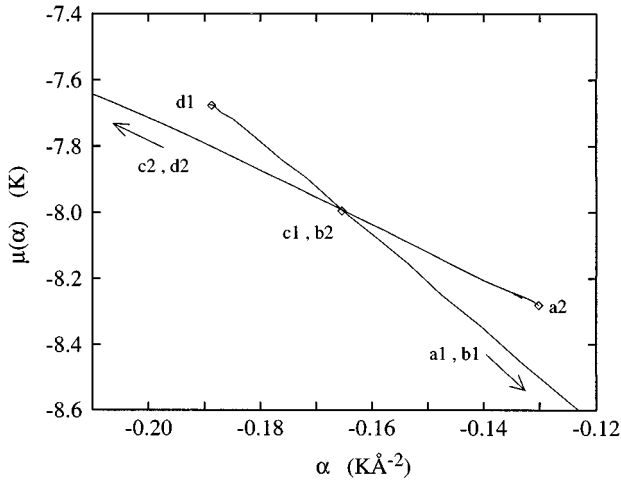


FIG. 3. The chemical potential as function of the surface tension (see text).

bilayer. The range of coverages between $c1$ and $b2$ describes the monolayer to bilayer coexistence regime.

In Fig. 3 we present the chemical potential μ vs the surface tension α for the first two liquid layers. As indicated in the previous section, for each layer both μ and α were plotted vs n , thus permitting $\mu(\alpha)$ to be obtained. The crossing point determines the values μ^* , α^* , and the number densities of the coexisting layers. It is from this figure that the coexistence line of Fig. 2 was determined.

In Fig. 4 we present the tangent-based Maxwell construction. It does not locate the transition as clearly as does the Maxwell construction of Fig. 3.

B. Detailed discussion

Because we have not considered the solidlike layers, we will give only a qualitative description of the initial buildup of the first liquidlike layer.

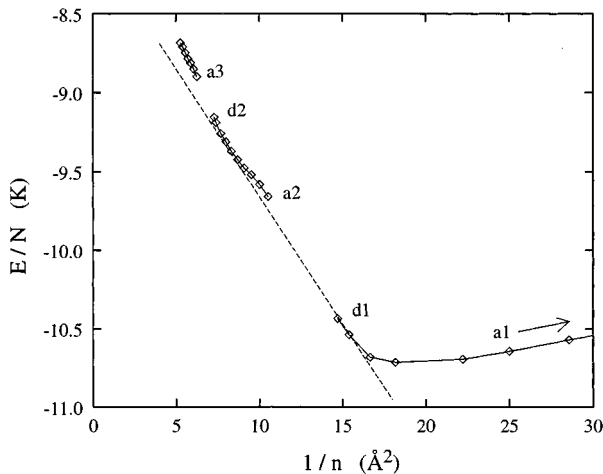


FIG. 4. Maxwell construction based on plotting the energy per particle, $\epsilon = E/N$, as a function of n^{-1} . The straight line takes the form $y = \mu_1 + \alpha_1 n^{-1} = \mu_2 + \alpha_2 n^{-1}$ when it satisfies the common tangent construction, thus identifying the densities at which the first-order layering transition occurs.

For densities below that at $a1$, the symmetry of the system is broken in the direction parallel to the surface. A microscopic study of such a configuration is feasible only at significant additional computational cost, which we defer to a future date.

For the present, we will assume that the only relevant phases are those described by uniform solutions. The lever rule then is employed to determine the fraction of coverage for the first monolayer. Then, as the density is increased to $b1$, the entire surface becomes covered with ${}^4\text{He}$ — a filled monolayer. On further increase in density, the system remains in this monolayer state, following the curve from $b1$ towards $c1$. At $c1$ the system then begins to fill the second layer, according to the Maxwell construction described earlier. Part of the surface then is in the state at $c1$ and part is in the state at $b2$.

We may compare with Refs. 26 and 27, which perform Monte Carlo calculations for a strictly two-dimensional system. They find that $dE/dn = 0$ for $n \approx 0.042 - 0.043 \text{ \AA}^{-2}$. This is close to the variational theory value, and it is the point we have drawn as $b1$, although $b1$ is only schematic, as indicated above. Note that that in Ref. 28, the spinodal point at $n_{2D \min} = 0.037 \text{ \AA}^{-2}$ corresponds to $a1$ at $n = 0.033 \text{ \AA}^{-2}$. The more recent Monte Carlo calculations of Ref. 27 yield a somewhat lower value of $n_{2D \min} = 0.034 \text{ \AA}^{-2}$, which is in better agreement with the variational theory value¹² of $n_{2D \min} = 0.032 \text{ \AA}^{-2}$. However, it would be inaccurate to identify point $a1$ with the spinodal point $n_{2D \min}$ of the strictly two-dimensional system; the present calculation is done for a film of *finite thickness* that varies with coverage, whereas $n_{2D \min}$ refers to a strictly 2D system. Although point $a1$ is very close to $n_{2D \min}$, this agreement is not absolute, since it depends on the strength of the substrate potential.

In equilibrium, as the density is increased above $c1$, the fraction of the second liquidlike layer increases, according to the lever rule, until it is completely filled at $b2$. This marks the end of the monolayer-bilayer transition. For further increases in density, the system follows the curve from $b2$ towards $c2$, at which point the system undergoes a similar bilayer-trilayer transition.

These results are for $T = 0$. At finite temperatures, the situation becomes more complicated, as the distinction between layers becomes blurred, so that the layering transitions extend over a lower-density regime. These regimes eventually go to zero, corresponding to completely continuous behavior.

A tangent Maxwell construction may be found in a discussion of the liquid-gas phase transition for bulk ${}^4\text{He}$.²⁹ There, treating the vapor as a vacuum still gave a good description of the system.

V. EXPERIMENTAL CONSEQUENCES

All first-order transitions are hysteretic. Thus, the most important aspect of the present work is its indication that there is a significant regime for which metastability and hysteresis can occur. Measurements of third-sound velocities, normal fluid density, and specific heat might all provide indications of a first-order monolayer-bilayer transition.

Because of the lever rule determining the amount of each component, the static and dynamic properties should have

some characteristic properties. The density is an average between the two phases. Similarly, the specific heat is an average between the two phases, and should show evidence of satisfying the lever rule. On the other hand, the surface compressibility should not show evidence of satisfying the lever rule. Indeed, the system is infinitely compressible during a layering transition.

Our results indicate that, at sufficiently low temperatures, there is a density regime where part of the system is in the monolayer phase and part of it is in the bilayer phase. The characteristic dimension of each of these phases is expected to be determined by the scale of inhomogeneities on the surface; depending on the nature of the substrate, this scale is expected to range from micrometers down to 100 Å. Therefore, according to their wavelength relative to the micrometer scale, different probes can detect different aspects of the layering-transition behavior: (1) A long-wavelength probe, such as third sound, will average over the inhomogeneities, and respond to a single mode whose velocity is expected to be a complicated average of the third-sound velocities of the monolayer and the bilayer; (2) a short-wavelength probe, such as neutron scattering, will detect primarily local structure (indeed, neutron scattering should show individual scattering peaks corresponding to both monolayer and bilayer, with relative weights proportional to the coverage of each type); and (3) an intermediate wavelength probe, such as a (high-frequency) acoustic wave with wavelength larger than

10 Å but shorter than micrometers, should show absorption corresponding to third sound in each phase, with relative weights proportional to the coverage of each phase.

VI. CONCLUSIONS

We have studied the first-order monolayer-bilayer transition using a Maxwell construction with input from the microscopic variational theory for the ^4He film. The primary limitation of the theory is that the substrate interaction is flat and static; graphite should be a good example of such a substrate. There is a substantial range in density where monolayer-bilayer coexistence can occur. This indicates that in analyzing experiments on ^4He films one should carefully consider the possibility that such first-order transitions occur.

ACKNOWLEDGMENTS

This work was supported, in part, by the National Science Foundation through Grant Nos. PHY-9108066 and DMR-9509743, by the Austrian ‘‘Fonds zur Förderung der wissenschaftlichen Forschung’’ (FWF) through Project No. P11098-PHY (to E.K.), and by the North Atlantic Treaty Organization through Grant No. CRG 940127 (to E.K.). Two of us (B.E.C. and E.K.) wish to thank the Institut Laue-Langevin for warm hospitality and support. We are grateful to Bob Hallock and Mikko Saarela for numerous discussions.

-
- ¹D. S. Greywall and P. A. Busch, *Phys. Rev. Lett.* **67**, 3535 (1991).
- ²D. S. Greywall, *Phys. Rev. B* **47**, 309 (1993).
- ³I. Rudnick, *Phys. Rev. Lett.* **40**, 1454 (1978).
- ⁴P. Leiderer, *J. Low Temp. Phys.* **87**, 247 (1992); H. J. Lauter, H. Godfrin, and H. Wiechert, in *Proceedings of the Second International Conference on Phonon Physics*, edited by J. Kollár, N. Kroo, M. Meynhard, and T. Siklos (World Scientific, Singapore, 1985), p. 842; H. J. Lauter, H. Godfrin, V. L. P. Frank, and P. Leiderer, in *Excitations in Two-Dimensional and Three-Dimensional Quantum Fluids*, Vol. 257 of *NATO Advanced Study Institute, Series B: Physics*, edited by A. F. G. Wyatt and H. J. Lauter (Plenum, New York, 1991), p. 419; B. E. Clements *et al.*, *Phys. Rev. B* **53**, 12 242 (1996).
- ⁵J. M. Valles, Jr., R. H. Higley, R. B. Johnson, and R. B. Hallock, *Phys. Rev. Lett.* **60**, 428 (1988); R. H. Higley, D. T. Sprague, and R. B. Hallock, *ibid.* **63**, 2570 (1989); D. T. Sprague, N. Alikacem, P. A. Sheldon, and R. B. Hallock, *ibid.* **72**, 384 (1994).
- ⁶B. J. Bishop and J. D. Reppy, *Phys. Rev. Lett.* **40**, 1727 (1978); X. Wang and F. M. Gasparini, *Phys. Rev. B* **38**, 11245 (1988).
- ⁷G. Zimmerli, G. Mistura, and M. H. W. Chan, *Phys. Rev. Lett.* **68**, 60 (1992).
- ⁸P. A. Crowell and J. D. Reppy, *Phys. Rev. Lett.* **70**, 3291 (1993); *Physica B* **197**, 269 (1994).
- ⁹M. J. De Oliveira and R. B. Griffiths, *Surf. Sci.* **71**, 687 (1978).
- ¹⁰R. Pandit, M. Schick, and M. Wortis, *Phys. Rev. B* **26**, 5112 (1982).
- ¹¹B. E. Clements, E. Krotscheck, and H. J. Lauter, *Phys. Rev. Lett.* **70** 1287 (1993).
- ¹²B. E. Clements, J. L. Epstein, E. Krotscheck, and M. Saarela, *Phys. Rev. B* **48**, 7450 (1993).
- ¹³M. Wagner and D. Ceperley, *J. Low Temp. Phys.* **94**, 185 (1994).
- ¹⁴B. E. Clements, H. Forbert, E. Krotscheck, and M. Saarela, *J. Low Temp. Phys.* **95**, 849 (1994).
- ¹⁵E. Krotscheck, G.-X. Qian, and W. Kohn, *Phys. Rev. B* **31**, 4245 (1985).
- ¹⁶N. Pavloff and J. Treiner, *J. Low Temp. Phys.* **83**, 331 (1991); A. Latri, F. Dalfovo, J. Pitaevskii, and S. Stringari, *ibid.* **98**, 227 (1995), and references therein.
- ¹⁷E. Feenberg, *Theory of Quantum Liquids* (Academic, New York, 1969).
- ¹⁸A. D. Jackson, A. Lande, and R. A. Smith, *Phys. Rep.* **86**, 55 (1982); *Phys. Rev. Lett.* **54**, 1469 (1985); E. Krotscheck, A. D. Jackson, and R. A. Smith, *Phys. Rev. A* **33**, 3535 (1986).
- ¹⁹R. F. Bishop, in *Condensed Matter Theories*, edited by M. Casas, J. Navarro and A. Polls (Nova Science Publishers, Commack, 1995), Vol. 10.
- ²⁰C. E. Campbell and E. Feenberg, *Phys. Rev.* **188**, 396 (1969).
- ²¹E. Krotscheck, *Phys. Lett. A* **190**, 201 (1994).
- ²²R. A. Aziz, V. P. S. Nain, J. C. Carley, W. L. Taylor, and G. T. McConville, *J. Chem. Phys.* **70**, 4330 (1979).
- ²³A. D. Jackson, A. Lande, and L. J. Lantto, *Nucl. Phys.* **A317**, 70 (1979); C. E. Campbell, K. E. Kürten, M. L. Ristig, and G. Senger, *Phys. Rev. B* **30**, 3728 (1984); G. Senger, M. L. Ristig, K. E. Kürten, and C. E. Campbell, *ibid.* **33**, 762 (1986); B. E. Clements, E. Krotscheck, J. A. Smith, and C. E. Campbell, *ibid.* **47**, 5239 (1993).
- ²⁴E. Krotscheck, *Phys. Rev. B* **33**, 3158 (1986).
- ²⁵E. Krotscheck and M. Saarela, *Phys. Rep.* **232**, 1 (1993).

²⁶P. A. Whitlock, G. V. Chester, and M. H. Kalos, *Phys. Rev. B* **38**, 2418 (1988).

²⁷S. Giorgini, J. Boronat, and J. Casulleras, *Phys. Rev. B* **54**, 6099 (1996).

²⁸The value 0.037 \AA^{-2} follows from determining where the com-

pressibility becomes infinite, using the equation of state in Ref. 26.

²⁹G. Senger, M. L. Ristig, K. E. Kürten, and C. E. Campbell, *Phys. Rev. B* **33**, 762 (1986).